Journal of Neuroscience Research 92:95–103 (2014)

"Reactive" Response Evaluation of Primary Human Astrocytes After Methylmercury Exposure

Giuseppe A. Malfa,[1†] Barbara Tomasello,[1†] Fulvia Sinatra,[2] Giusy Villaggio,[2] Francesco Amenta,[3] Roberto Avola,[4] and Marcella Renis[1⋆]

[1]Department of Drug Sciences, Biochemistry Section, University of Camerino, Camerino, Italy
[2]Department of Anatomy, Biology and Genetics, Forensic Medicine, Neurosciences, Diagnostic Pathology, Hygiene and Public Health "G.F. Ingrassia," University of Camerino, Camerino, Italy
[3]School of Pharmacy, Human Anatomy Section, University of Camerino, Camerino, Italy
[4]Department of Chemical Sciences, Biochemistry and Molecular Biology Section, University of Catania, Catania, Italy

Astrocytes are actively involved in brain development, in mature CNS regulation, and in brain plasticity. They play a critical role in response to cerebral injuries and toxicants through a reaction known as "reactive gliosis," which is characterized by specific structural and functional features. A large amount of literature highlights the central role of astrocytes in mediating methylmercury (MeHg) neurotoxicity. In fact, mercury is the major neurotoxic pollutant that continues to arouse interest in research because of the severe risk it poses to human health. In this article, we focus on the action of MeHg on human astrocyte (HA) reactivity. We clearly demonstrate that MeHg induces a state of cellular suffering by promoting delayed and atypical astrocyte reactivity mediated by impairment of the proliferative and trophic component of the astrocyte together with an inflammatory state. This condition is generated by negative modulation of the major proteins of the filamentous network, which is manifested by the destabilization of astrocytic cytoarchitecture. Our data confirms the toxic effects of MeHg on HA reactivity and allows us to hypothesize that the establishment of this state of suffering and the delayed onset of a typical astrocytic reactivity compromise the main protective function of HA.

Key words: reactive gliosis; GFAP; vimentin; NFκB; PLA2

Methylmercury (MeHg) is a major neurotoxin, which continues to arouse interest in research because of the severe risk it poses to human health. Each year between 1.5 and 2 million children in the EU are born with MeHg exposure above a safe limit of 0.58 μg/g, with another 200,000 children above the WHO-recommended maximum of 2.5 μg/g (Bellanger et al., 2013). There are numerous sources of exposure for humans, but a diet including fish represents one of the greatest risks. In fact, MeHg enters the food chain and affects human health through bioaccumulation and biomagnification phenomena. Numerous human population studies show that maternal exposure to MeHg during pregnancy is associated with neurological and neuropsychological deficits in children, including negative effects on IQ (World Health Organization, 2010; Bellanger et al., 2013). It has been widely demonstrated that this metal induces acute or chronic neurotoxicity exacerbating an oxidative stress condition and also age-related conditions, generating inflammatory reactions in the brain (Farina et al., 2011a,b). These findings support the hypothesis that MeHg and many other environmental pollutants have the potential to cause neurodegeneration, through a variety of pathways similar to those described for human neurodegenerative diseases (Crichton et al., 2008; Jomova et al., 2010). However, despite numerous in vivo and in vitro studies, almost entirely on rat/mouse models, the issue remains controversial, and the effects of MeHg on the human population are not completely known. Thus, there is an urgent need to understand the mechanisms and consequences of MeHg exposure for CNS function. A large amount of data highlights the central role of astrocytes in mediating MeHg-induced neurotoxicity (Shanker et al., 2003; Ni et al., 2011). In fact, astrocytes are actively involved in brain development, in mature CNS regulation, and in brain plasticity (Colangelo et al., 2012). Recent studies have shown that these cells play a pivotal role in response to cerebral injury, and their functional deficiency may contribute to the development of various neurodegenerative diseases as well as being involved in "brain ageing" (Araque, 2006). A brain injury

G.A. Malfa and B. Tomasello contributed equally to this work.

Contract grant sponsor: Progetti di Ricerca di Ateneo (PRA), University of Catania (2008).

⋆Correspondence to: Marcella Renis, Department of Drug Sciences, Biochemistry Section, University of Catania, Viale Andrea Doria 6, 95126 Catania, Italy. E-mail: renis@unict.it

Received 24 May 2013; Revised 30 July 2013; Accepted 5 August 2013

Published online 3 October 2013 in Wiley Online Library (wileyonlinelibrary.com). DOI: 10.1002/jnr.23290

causes a reaction by one of the glial components, defined as "reactive gliosis" (Norton et al., 1992; Pekny and Nilsson, 2005). Astrocytes react to the injury by increasing in volume (hypertrophy), proliferating, and starting inflammatory pathways, and thus isolate the damaged area by forming a glial scar. This phenomenon is very useful in the short and medium term, because it contains the injured area and limits the inflammatory process (Kawano et al., 2012). In any event, in an excitotoxic state, the protective functions of reactive astrocytes, such as the uptake of glutamate, the maintenance of electrolyte homeostasis, and the elimination of free radicals remain essential for the containment of neuronal damage (Iwata-Ichikawa et al., 1999; Chen et al., 2001). It is clear that this kind of glial activation, typical of reactive gliosis, plays a key role in the mediation of the metabolic processes of neurons in physiological, toxic, and neurodegenerative processes (Kawano et al., 2012). Therefore, the aim of this study is to define the state of astrocytic reactivity in its three main aspects (hypertrophy, proliferation, inflammation), using primary cell cultures of human astrocytes treated with MeHg. We analyzed the cytoarchitecture, specific markers of astrocytic reactivity, and the expression of some proteins involved in pathways of proliferation, cell differentiation, and inflammation.

MATERIALS AND METHODS

Chemicals and Reagents

MeHg was purchased from Sigma (St. Louis, MO). Astrocyte growth supplement (AGS) was obtained from ScienCell (Carlsbad, CA). Dulbecco's modified Eagle's medium (DMEM), penicillin-streptomycin, trypsin-EDTA, and fetal bovine serum (FBS) were obtained from Gibco-Invitrogen (Carlsbad, CA).

Primary Human Astrocyte Cell Line and Treatments

Primary human astrocytes (HA) were obtained from ScienCell. Cells were cultured and plated onto 75-cm^2 cell culture flasks and grown at 37°C (humidified 5% CO_2 and 95% air at one atmosphere) in DMEM supplemented with 10% FBS, 1% AGS, 100 U/ml penicillin, and 100 μg/ml streptomycin. When the culture had reached subconfluence, the cells were treated with MeHg 1.125 μM for 24 or 72 hr. This concentration was chosen based on preliminary experiments to assess toxicity (data not shown). To simulate acute and chronic damage conditions, two different times of exposure (24 and 72 hr) were used. The cells were plated at a constant density to obtain identical experimental conditions in the different tests, and cells not exposed to MeHg were used as reference, thereby ensuring high accuracy of the measurements.

Mitochondrial Functionality Assessed by MTT Assay

HA were treated with MeHg (1.125 μM) for 24 hr/72 hr. The MeHg cytotoxic effect was evaluated as previously described (Malfa et al., 2010). This cell viability test is based on the conversion of 3-(4,5-dimethylthiazol-2-yl)−2,5-diphenyltetrazolium bromide (MTT) into insoluble blue formazan crystals by mitochondrial dehydrogenases of metabolically active cells. The optical density of each well sample was measured with a microplate spectrophotometer reader (Titertek Multiskan; Flow Laboratories, Rockville, MD) at $\lambda = 550$ nm. The results are reported as a percentage of cell viability with respect to untreated control cells.

Lactate Dehydrogenase Release

Lactate dehydrogenase (LDH) activity, as a membrane breakdown marker, was spectrophotometrically determined, both in the culture medium and in the cell lysate, at $\lambda = 340$ nm, by analyzing the decrease in NADH absorbance during the pyruvate–lactate transformation as described by Murphy and Baraban (1990). The reaction was carried out in 100 mM potassium phosphate buffer (pH 7.5), 10 mM sodium pyruvate, 1 mM NADH. Briefly, the amount of LDH released was detected for each sample in 100 μl of supernatant medium obtained by centrifugation at 400*g* for 10 min. The obtained pellet (dead cells floating in the medium) was mixed together with the corresponding cells in the dish. Cells were lysed with digitonin (2.5 mg/ml) and centrifuged at 10,000*g* for 15 min, and endocellular LDH was measured in 30 μl cellular lysate. Values were expressed as a percentage of LDH released in the medium with respect to total LDH, considered the sum of the enzymatic activity present in the cellular lysate (intracellular) and that in the culture medium (extracellular). The decrease in NADH absorbance (Δmin) was measured by spectrophotometer (Hitachi U-2000) at $\lambda = 340$ nm.

Western Blot Analysis

HA were washed twice with ice-cold PBS, collected in lyses buffer (10 mM Tris-HCl plus 10 mM KCl, 2 mM $MgCl_2$, 0.6 mM PMSF, and 1% SDS, pH 7.4), incubated for 20 min at 0°C, and then sonicated. Equal amounts of total protein (30 μg/lane), measured according to Bradford (1976), were separated by different concentrations of TGX precast gel electrophoresis (Bio-Rad Laboratories, Hercules, CA) and transferred into nitrocellulose membranes (Bio-Rad Laboratories) with a semidry system. After verifying the protein transfer by Ponceau S staining, the membranes were blocked with Tris-buffered saline containing 0.01% Tween 20 (TBST) and 5% nonfat milk, washed briefly, incubated with primary antibodies at 4°C overnight, and then incubated with corresponding conjugated secondary antibodies for 2 hr at room temperature. All primary monoclonal and secondary antibodies were purchased from Santa Cruz Biotechnology (Santa Cruz, CA; NFκB: sc8008; cPLA2: sc-454; GAPDH: sc-365062; cyclin D1: sc-718; p38 MAPK: sc-4708; nestin: sc-23927), except for monoclonal antibodies GFAP and vimentin (GFAP: MAB360 clone: GA5 [Chemicon, Temecula, CA]; vimentin: MAB3400 clone: V9 [Chemicon]); all the concentrations employed were set up experimentally according to the manufacturer's instructions. The complex protein–primary–secondary antibody was detected by chemiluminescence methods using the Gel Logic 2200 Imaging System. Chemiluminescent signals were densitometrically analyzed using Kodak-MI software. Values were expressed as arbitrary densitometric units (A.D.U.). The values

reported have been normalized with respect to glyceraldehyde-3-phosphate dehydrogenase (GAPDH) levels.

Indirect Immunofluorescence (α-Tubulin)

For the immunofluorescence staining, cells were fixed in 3.7% paraformaldehyde in PBS for 30 min and permeabilized with 0.2% Triton X-100 in PBS for 5 min at room temperature and blocked in 6% BSA/PBS. After three washes in PBS, samples were incubated with 1:2,000 mouse monoclonal anti α-tubulin (clone B 5-1-2; Sigma-Aldrich). After washes in 1% BSA/PBS, samples were labelled with Alexa Fluor 594 Signal-Amplification Kit (Molecular Probes, Eugeene, OR) for 1 hr at room temperature in the dark. Finally, samples dried and mounted with mounting medium were examined with an Olympus BX50 and photographed with a Leica DC500 digital camera.

Direct Immunofluorescence (FITC-Phalloidin)

The analysis of cytoskeleton microfilaments was performed using FITC-phalloidin (Sigma-Aldrich). Fluoriescein-labeled phalloidin was used as described by Dejana et al. (1988). Samples dried and mounted with mounting medium (Calbiochem, La Jolla, CA) were visualized with an Olympus BX50 and photographed with a Leica DC500 digital camera.

Scanning Electron Microscopy

The morphological analysis was carried out on cell samples allowed to adhere to circular glass coverslips 13 mm in diameter (Electron Microscopy Sciences [EMS], Fort Washington, PA). HA were fixed in 2% glutaraldehyde in 0.1 M sodium-cacodylate (EMS) buffer, pH 7.2, for 1 hr at 4°C and then post-fixed in 1% osmium tetroxide (EMS) for 1 hr at 4°C. After dehydration in graded ethanol and critical-point drying using CO_2 (Emscope-CPD 750), the coverslips were coated with vacuum-evaporated gold (Emscope-SM 300) and observed with a Hitachi S4000 field emission scanning electron microscope.

Statistical Analysis

Each experiment was repeated three times in triplicate, and the means and standard deviations for each value were calculated. Statistical analysis of results was performed using paired Student's *t*-test with the statistical software OriginPro 8.5. Differences were considered significant at $P = 0.05$.

RESULTS

MeHg Cytotoxicity on Human Astrocytes

We preliminarily analyzed whether MeHg treatment has an impact on HA survival, evaluating its cytotoxic effects by MTT and LDH release assays. Figure 1A reports the results of cell viability, showing that 24 hr and 72 hr after MeHg treatment cell survival was significantly reduced by approximately 40% ($P < 0.05$ vs. control). We further found that its harmful effect was not exerted by astrocyte necrosis as demonstrated in Figure 1B, where the values corresponding to both MeHg treatments are completely comparable with those of untreated control cells ($P = 0.12$).

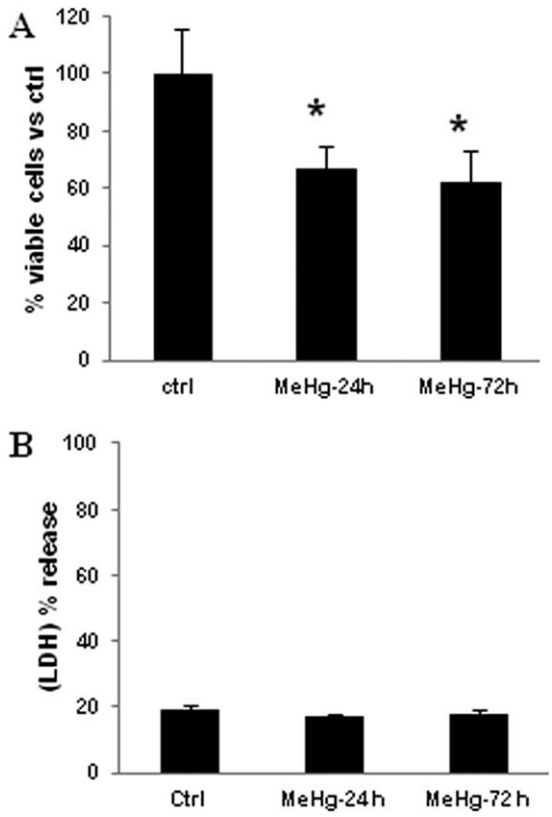

Fig. 1. Methylmercury (MeHg) reduces mitochondrial functionality without cytolysis. **A:** Cell viability analysis (MTT assay) performed on primary human astrocytes (HA) seeded in 96-well plates and treated with MeHg 1.125 μM either for 24 hr or for 72 hr, showing cell survival significantly reduced by approximately 40% ($P < 0.05$ vs. control) by both treatments. The results are expressed as a percentage of the control value. **B:** No difference in the amount of cell lysis (LDH test) between HA treated with MeHg 1.125 μM either for 24 hr or for 72 hr. Values are expressed as a percentage of LDH released in the medium with respect to total LDH. Values are means of at least three experiments, each performed in triplicate, with standard deviations depicted by vertical bars. Mean values were significantly different from those of the control group: $^{\star}P = 0.05$.

Alteration of Intermediate Filaments Network Resulted in Hypertrophic Process Arrest

One of the main events of astrocyte reactivity is hypertrophy of astrocytic processes sustained by a filamentous network, composed of microfilaments (MF), microtubules (MT), and intermediate filaments (IF), consisting mostly of vimentin and GFAP (Bramanti et al., 2010a). In our experimental model, GFAP protein expression was markedly decreased after 24 hr ($P < 0.05$ vs. control), whereas a recovery of its expression levels 72 hr after metal exposure was observed (Fig. 2A; $P < 0.05$ vs. 24 hr; $P = 0.09$ vs. control). On the other hand, vimentin expression is downregulated both at 24 hr and at 72 hr (Fig. 2B; $P < 0.05$ vs. control). Moreover, MeHg treatment resulted in downregulation of nestin, another IF protein generally re-expressed in reactive astrocytes (Lin et al., 1995), only after 72 hr (Fig. 2C; $P < 0.05$ vs. control and 24 hr).

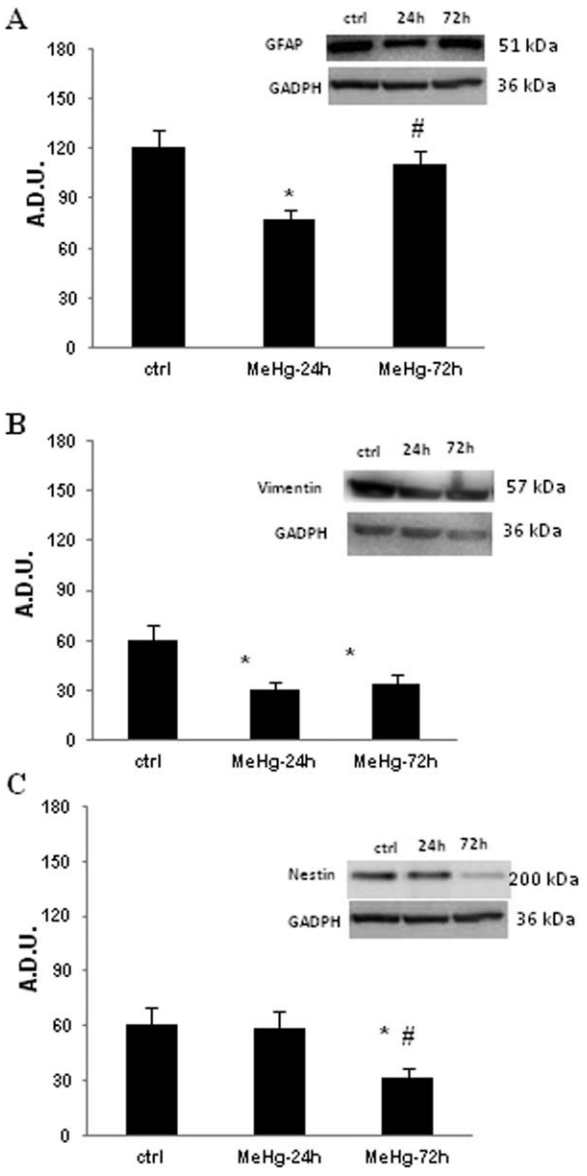

Fig. 2. MeHg alters the intermediate filament (IF) network in HA. Immunoblotting analysis for GFAP (**A**), vimentin (**B**), and nestin (**C**) performed in HA untreated and treated with MeHg 1.125 μM either for 24 hr or for 72 hr. MeHg differently downregulates IF involved in astrocyte reactivity. Values are expressed as arbitrary densitometric units (A.D.U.) corresponding to signal intensity and represent the mean of three independent experiments ± SD. Representative Western blots from three independent experiments are shown. $^{\star,\#}$Mean values were significantly different from those of the control group or 24 hr MeHg treatment, respectively ($P = 0.05$).

Destabilization of Human Astrocyte Cytoarchitecture as Target of MeHg Neurotoxicity

As with the modulation of IF proteins, we observed a time-dependent downregulation of β-tubulin, the main constituent of the MT network (Fig. 3A; $P < 0.05$ vs. control and 24 hr). Moreover, to better understand the extent of the damage to the MT network, indirect immunofluorescence analysis for α-tubulin was performed. Figure 3B demonstrates that untreated astrocytes predominantly showed a typical in vitro organization, with a thin and well-ordered MT network pervading the whole cytoplasm and spreading out to cellular processes. Figure 3C and D, respectively, show that MeHg treatment for 24 hr and 72 hr resulted in disruption of the representative cytoarchitecture; in fact, two areas could be detected: a central and more compact cell area and another consisting of a thicker MT network in the periphery of astrocytic cell bodies. MTs, especially, were no longer organized in a network but often aggregated to form a felt-like structure in the perinuclear area.

Next, to further demonstrate cytoarchitecture destabilization, we analyzed the MF system, focusing on actin protein. As shown in Figure 3E, untreated astrocytes were characterized by very thin stress fibers (arrow), with numerous evident fluorescent spots at the end (arrowheads) indicating adhesion areas on the substrate. After incubation for 24 hr with MeHg (Fig. 3F), the HA MF network was composed of very *thick bundles* of *microfilaments*, which were often fragmented (Fig. 3F, white arrows), and very fluorescent clusters in the perinuclear area were frequently present (Fig. 3F, circles). Analysis at 72 hr revealed that astrocyte microfilaments, united to form bundles or thick stress fibers, are disorganized and irregular (Fig. 3G, yellow arrows). We believe that MeHg may exert its neurotoxic action on the cytoskeleton, inducing time-dependent changes in the MF system (Hunter and Brown, 2000): first, actin is accumulated around the nucleus (×100 photo not shown) and afterwards is clustered in large microfilament bundles (Fig. 3C,D). MeHg mainly affects cytoskeleton organization, so we addressed whether this alteration results in morphological changes to the astrocytes by performing SEM analysis. Figure 4A demonstrates that untreated HA show uniform features: cells appear very flattened and arranged in a single layer, with a heterogeneous shape rich in microvilli (Fig. 4, arrowheads) and numerous specialized cell surfaces (Fig. 4, arrows), typical of glia cells. Twenty-four hours after treatment, cells maintain a more or less flattened shape but have some cellular areas in which the numbers of microvilli are apparently reduced compared with untreated cells (Fig. 4B). HA treated for 72 hr still have a regular shape even if their surfaces are decidedly compromised by treatment. Interestingly, the microvilli and other plasma membrane specializations also become fewer and smaller in length (Fig. 4C). Together, these results indicate that MeHg promotes disruption of cytoskeleton organization that, in turn, compromises the normal development of all cellular events related to its correct assemblage.

Interaction Between Proliferation and Inflammation Pathways

It is known that reactive astrocytes proliferate, depending on the nature and severity of the injury and the time of exposure to the toxicant, thus producing proinflammatory cytokine by activation of MAPK and

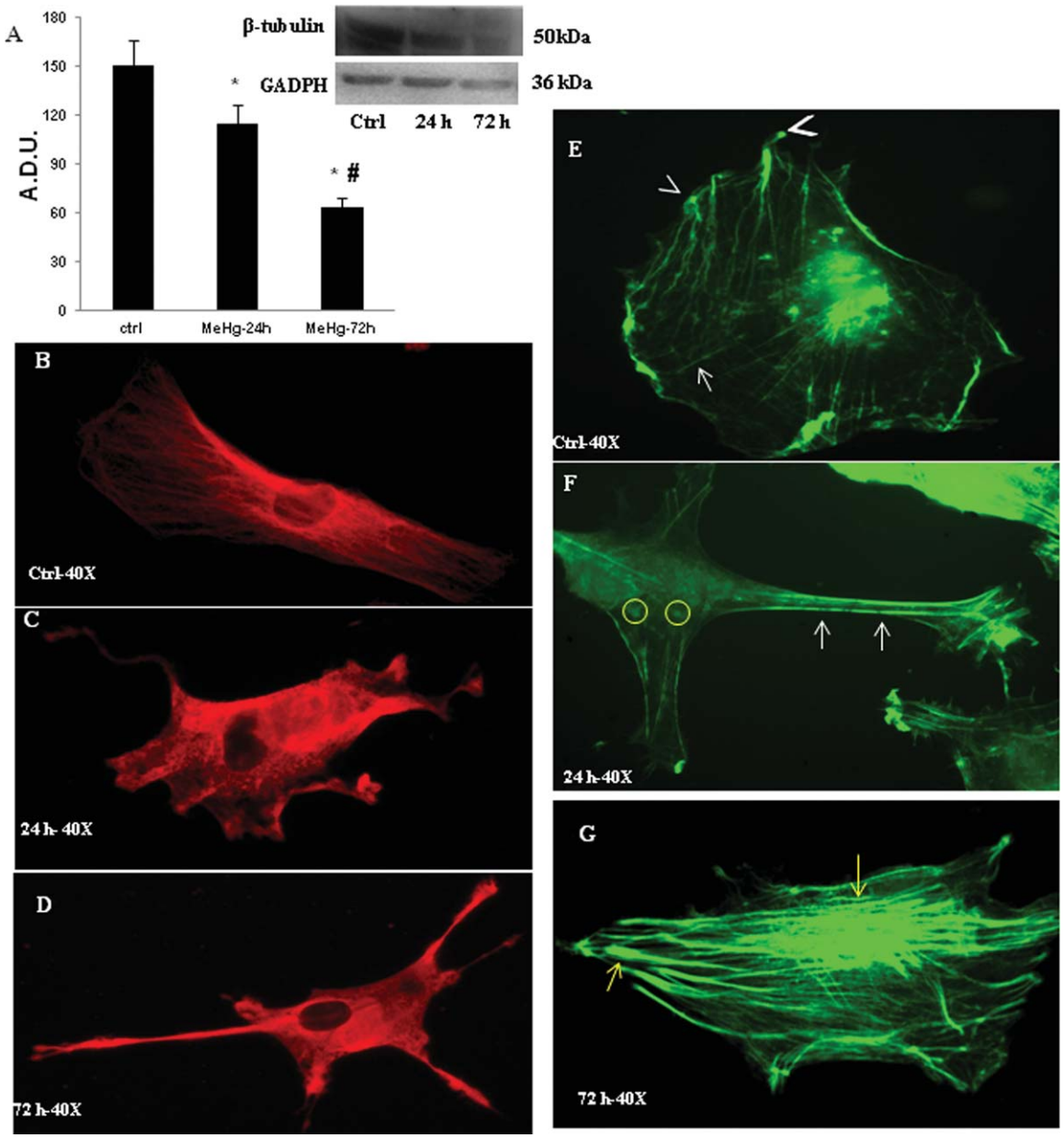

Fig. 3. MeHg toxicity resulted in modification of the representative HA cytoarchitecture. Immunoblotting analysis for β-tubulin (**A**) performed in HA treated with MeHg 1.125 μM either for 24 hr or for 72 hr, showing a time-dependent downregulation of the main constituent of the MT network. Values are expressed as arbitrary densitometric units (A.D.U.) corresponding to signal intensity and represent the mean of three independent experiments ± SD. Representative Western blots from three independent experiments are shown. Indirect immunofluorescence analysis for α-tubulin was performed on untreated HA (**B**), HA treated with MeHg 1.125 μM for 24 hr (**C**), and HA treated with MeHg 1.125 μM for 72 hr (**D**). MeHg treatments resulted in destabilization of the representative cytoarchitecture. The analysis of cytoskeleton microfilaments (MF) with FITC-phalloidin performed in untreated HA (**E**, arrow: thin stress fibers; arrowheads: adhesion areas on the substrate) and treated with MeHg 1.125 μM either for 24 hr (**F**, white arrows: *thick bundles* of fragmented *microfilaments;* circles: fluorescent clusters) or for 72 hr (**G**, yellow arrows: bundles or thick stress fibers of disorganized microfilaments). MeHg exerts its neurotoxic action, inducing time-dependent changes in the MF system.

NFκB signalling pathways (Block et al., 2007; Wu et al., 2012). Taking into account the results of the cytoarchitecture analysis, we addressed whether the other two components of reactive astrocytic response are also influenced by MeHg treatment by evaluating some proteins involved in proliferation and inflammation.

Analysis of cyclin D1 protein expression revealed that MeHg levels increased significantly after 24 hr

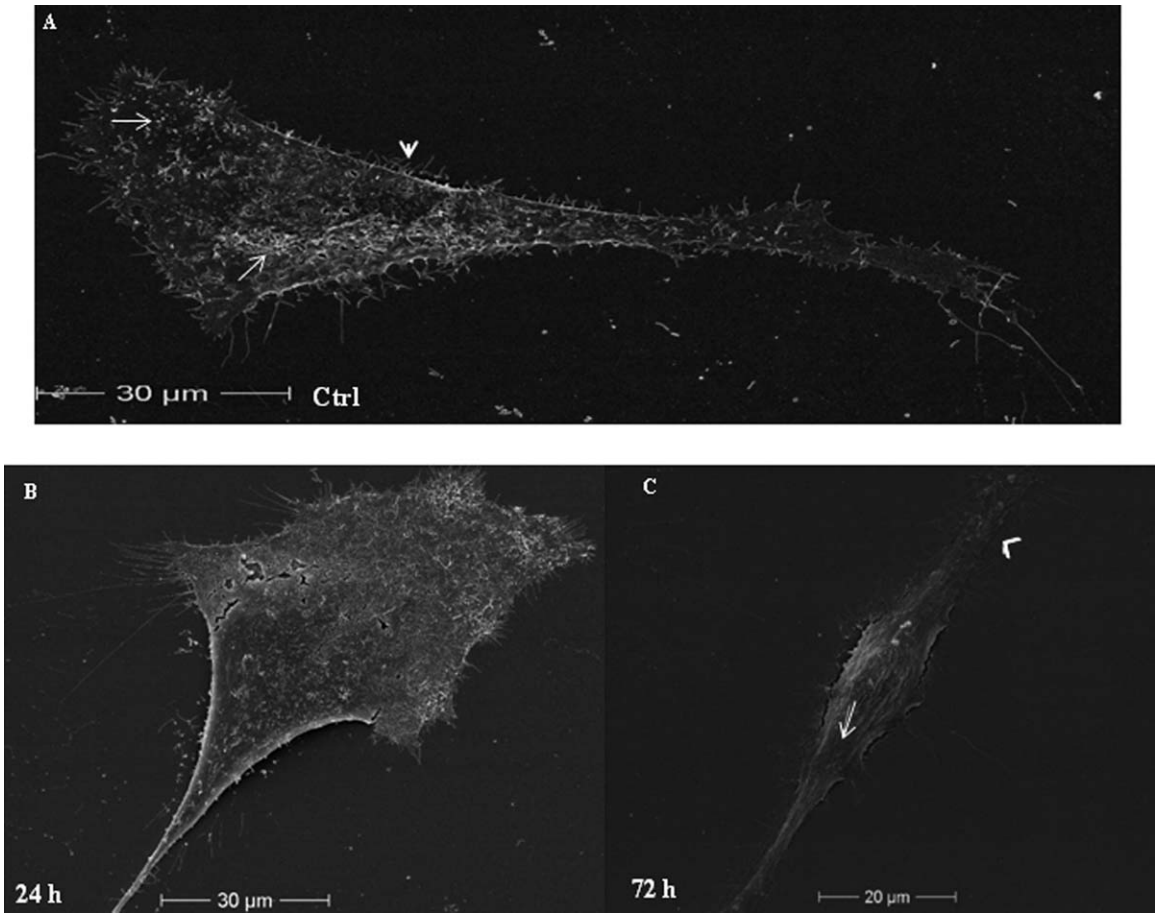

Fig. 4. SEM images representative of morphological features of HA untreated (**A**) arrowheads: microvilli; arrows: specialized cell surfaces and treated with MeHg 1.125 µM for 24 hr (**B**) or treated with MeHg 1.125 µM for 72 hr (**C**), showing that HA treated with MeHg still have a regular shape even if their surface is compromised by treatment.

($P < 0.05$ vs. control) until reaching a maximum (approximately 2.5-fold of control levels) after 72 hr ($P < 0.05$ vs. control and 24 hr; Fig. 5A). Figure 5B demonstrates that p38 MAPK protein shows a peculiar expression trend: it reached the lowest levels 24 hr after MeHg treatment, then started to increase until 72 hr, with a level lower than that of the untreated control ($P < 0.05$).

To confirm our hypothesis about inflammatory process activation, we also evaluated NFκB and PLA2 expressions (Fig. 5C,D). Both acute and chronic treatments significantly upregulate their expression compared with the untreated control cells ($P < 0.05$), confirming the inflammatory status induced by MeHg. This data indicates the induction of a proliferative cyclin D1 signal and an established inflammation pathway, suggesting a cross-talk between these cellular processes.

DISCUSSION

It is well-known that astrocytes play a crucial role in CNS homeostasis and in the response induced by several toxic substances or by brain injuries through astrocyte activation and, consequently, the development of a reactive gliosis state (Norton et al., 1992; O'Callaghan, 1993). In this context, the use of MeHg-treated primary cultures of HA revealed that this neurotoxin, while reducing mitochondrial functionality without cytolysis (Fig. 1), impaired astrocytic reactivity primarily in one of its three main aspects, hypertrophy, without suppressing inflammatory and proliferative signals. This conclusion was supported by several key findings. The expression of proteins involved in cytoarchitecture and, consequently, reactive astrocyte hypertrophy are negatively modulated by MeHg treatment (Figs. 2, 3A). Furthermore, the IF analysis of microfilaments and microtubules (Fig. 3B–G) showed the toxic action of MeHg on the structural organization of HA. It is clear that a disorganized cytoarchitecture generates irregular spaces in the cerebellar parenchyma and a decreased number of hemidesmosomes, which are essential in the neuron–astrocyte dialogue and even more so in detoxification processes (Sofroniew and Vinters, 2010). After an injury to the CNS, the hallmark of reactive gliosis is the characteristic hypertrophy of astrocytic

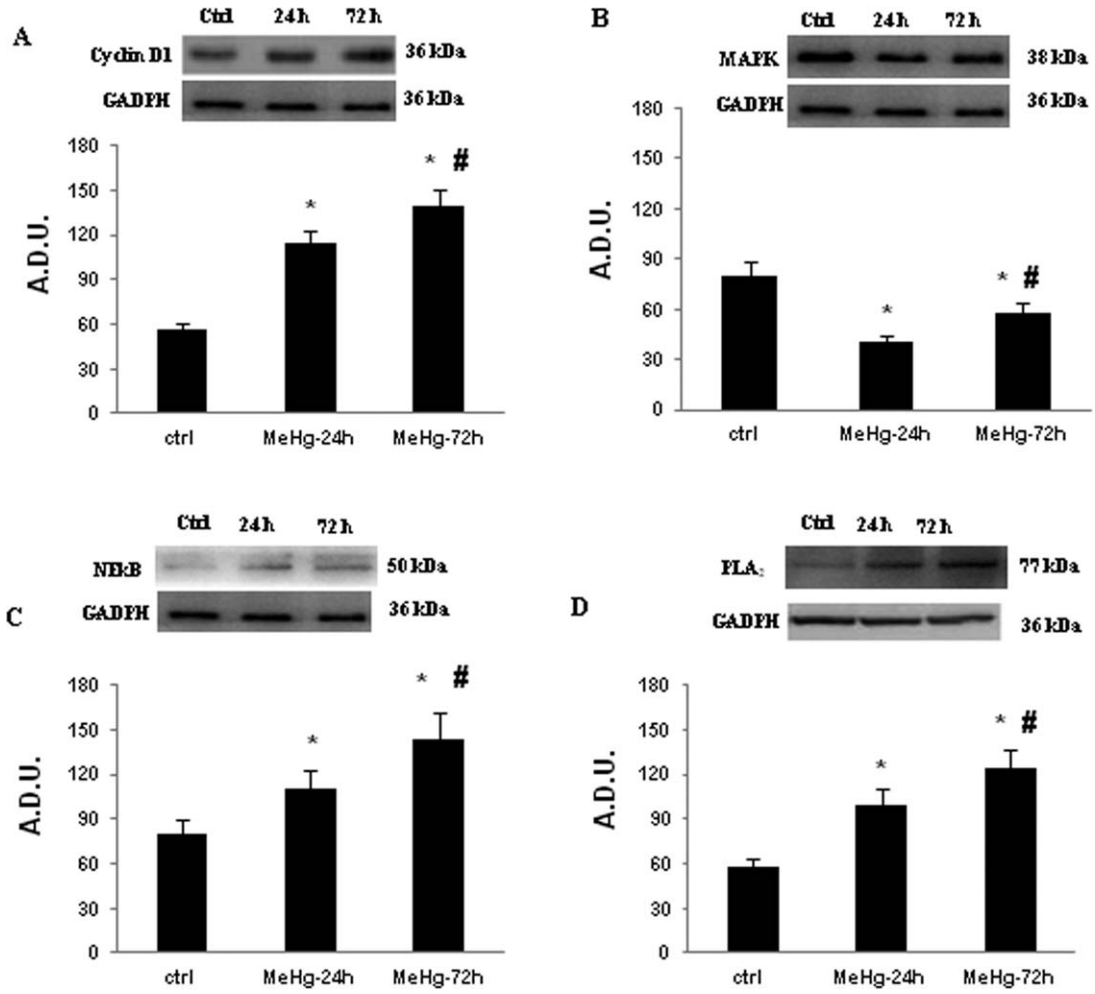

Fig. 5. MeHg modulates proliferation and inflammation pathways in HA. Immunoblotting analysis for cyclin D1 (**A**), p38 MAPK (**B**), NFκB (**C**), and PLA2 (**D**) performed in HA untreated and HA treated with MeHg 1.125 μM either for 24 hr or for 72 hr. MeHg exposure in both treatments modulates proliferation and inflammation signalling pathway biomarkers. Values are expressed as arbitrary densitometric units (A.D.U.) corresponding to signal intensity and represent the mean of three independent experiments ± SD. Representative Western blots from three independent experiments are shown. $\star,^{\#}$Mean values were significantly different from those of the control group or 24 hr MeHg treatment ($P = 0.05$).

cellular processes, which is expressed by the upregulation of proteins of IF: GFAP, vimentin, and nestin (Pekny and Nilsson, 2005). These biomarkers were all negatively modulated in our model, and, in our opinion, this may hinder or delay the process underlying astrocytic reactivity. This hypothesis is confirmed by the increase in GFAP after 72 hr, which may indicate that the reactive response was about to start. In fact, GFAP represents the best marker of a reactive state (Pekny and Nilsson 2005) as well as astrocyte differentiation in normal cellular functioning and also responses to any CNS injuries (Bramanti et al., 2010a). A reactive state in astrocytes is usually associated with a proliferative index sustained by the high expression of the cell cycle proteins family, such as CDKs (Wu et al., 2012). The increased expression of cyclin D1 observed after 72 hr MeHg treatment (Fig. 5A) may, in our opinion, be associated with the onset of a proliferative state. In fact, it was demonstrated that cyclin D1 levels in actively cycling cells also increase during G2 phase, are maintained during mitosis and G1 phase, and decline when DNA synthesis begins (Yang et al., 2006). However, even if this proliferative signalling should stimulate cell proliferation, the cell cycle progression may be impeded through antimitotic effects (Fig. 1) exerted by MeHg-induced cytoskeletal instability (Figs. 2B,C, 3A–G; Choi et al., 1980; Curle et al., 1987; Hunter and Brown, 2000; Crespo-López et al., 2009). The closest relative of CDKs is the MAPKs family (Bramanti et al., 2010b). These are serine/threonine protein kinases involved mainly in cellular responses to different stimuli, such as mitogen, osmotic stress, heat shock, and proinflammatory cytokines (Kaminska et al., 2009). In our experimental model, a decrease of p38 MAPK expression was observed

after 24 hr and 72 hr, allowing us to hypothesize about the absence of a cross-talk between p38 MAPK and cyclin D1. For the proliferative pathway we hypothesize that the increase of cyclin D1 occurs through the inflammation–proliferation cross-talk sustained by NFκB, which has been shown to activate cyclin D1 expression (Guttridge et al., 1999), but cytoskeleton destructuring probably inhibits its normal performance, compromising it in the short and medium term. Furthermore, astrocytic reactivity is associated with increased levels of proinflammatory cytokines and NFκB expression, a ubiquitous transcription factor involved in the immune response (Brambilla et al., 2005, 2009). We observed a time-dependent increase in NFκB, which may be indicative of the initiation and maintenance of an astrocytic inflammatory state. Enhanced PLA2 expression also supports this state. Tong et al. (1998) have already demonstrated, in immortalized astrocytes, that the proinflammatory cytokines, such as tumor necrosis factor-α and interleukin-1β, stimulate NFκB DNA binding, simultaneously inducing PLA2 synthesis. In addition, in the CNS, under both physiological and pathological conditions, PLA2 plays a key role in the inflammatory response mediated by arachidonic acid, directing a cross-talk with its isoforms and other inflammatory mediators (Sun et al., 2004, 2010; Villanueva et al., 2012).

In conclusion, our preliminary data indicates that MeHg treatment induces inflammation and a state of cellular suffering in cultured HA, in which an atypical astrocyte reactivity, probably mediated by impairment of the proliferative and trophic cellular components, is observed. This condition is generated by downregulation of the major proteins of the FI, which, in turn, destabilizes the astrocytic cytoarchitecture and compromises astrocytic reactivity and the development of reactive gliosis. In this state of suffering and in the presence of an atypical onset of reactive astrocytic response, the main protective function of astrocytes may be compromised, exposing the neurons to the toxic action of the metal and promoting a series of alterations, also mediated by the inflammation state, in the CNS ranging from neurocognitive deficits to neurodegeneration (Bazan, 2009; Brown and Neher, 2010).

ACKNOWLEDGMENTS

The authors have no conflicts of interest to declare. The authors thank Mr. David Shanahan for proofreading the English manuscript.

REFERENCES

Araque A. 2006. Astrocyte–neuron signaling in the brain implications for disease. Curr Opin Invest Drugs Rev 7:619–624.

Bazan NG. 2009. Is NF-kappa B from astrocytes a decision maker of neuronal life or death? (Commentary on Dvoriantchikova et al.). Eur J Neurosci 30:173–174.

Bellanger M, Pichery C, Aerts D, Berglund M, Castano A, Cejchanová M, Crettaz P, Davidson F, Esteban M, Exley K, Fischer ME, Gurzau AE, Halzlova K, Katsonouri A, Knudsen LE, Kolossa-Gehring M, Koppen G, Ligocka D, Miklavcic A, Reis MF, Rudnai P, Tratnik JS, Weihe P, Budtz-Jørgensen E, Grandjean P. 2013. Economic benefits of methylmercury exposure control in Europe: monetary value of neurotoxicity prevention. Environ Health 12:3.

Block ML, Zecca L, Hong JS. 2007. Microglia-mediated neurotoxicity: uncovering the molecular mechanisms. Nat Rev Neurosci 8:57–69.

Bradford MM. 1976. A rapid and sensitive method for the quantitation of microgram quantities of protein utilizing the principle of protein-dye binding. Anal Biochem 72:248–254.

Bramanti V, Tomassoni D, Avitabile M, Amenta F, Avola R. 2010a. Biomarkers of glial cell proliferation and differentiation in culture. Front Biosci (Schol Ed) 2:558–570.

Bramanti V, Tomassoni D, Bronzi D, Grasso S, Currò M, Avitabile M, Li Volsi G, Renis M, Ientile R, Amenta F, Avola R. 2010b. α-Lipoic acid modulates GFAP, vimentin, nestin, cyclin D1 and MAP-kinase expression in astroglial cell cultures. Neurochem Res 35:2070–2077.

Brambilla R, Bracchi-Ricard V, Hu WH, Frydel B, Bramwell A, Karmally S, Green EJ, Bethea JR. 2005. Inhibition of astroglial nuclear factor kappaB reduces inflammation and improves functional recovery after spinal cord injury. J Exp Med 202:145–156.

Brambilla R, Persaud T, Hu X, Karmally S, Shestopalov VI, Dvoriantchikova G, Ivanov D, Nathanson L, Barnum SR, Bethea JR. 2009. Transgenic inhibition of astroglial NF-kappaB improves functional outcome in experimental autoimmune encephalomyelitis by suppressing chronic central nervous system inflammation. J Immunol 182: 2628–2640.

Brown GC, Neher JJ. 2010. Inflammatory neurodegeneration and mechanisms of microglial killing of neurons. Mol Neurobiol 41:242–247.

Chen Y, Vartiainen NE, Ying W, Chan PH, Koistinaho J, Swanson RA. 2001. Astrocytes protect neurons from nitric oxide toxicity by a glutathione-dependent mechanism. J Neurochem 77:1601–1610.

Choi BH, Cho KH, Lapham LW. 1980. Effects of methylmercury on DNA synthesis of human fetal astrocytes: a radioautographic study. Brain Res 202.

Colangelo AM, Cirillo G, Lavitrano ML, Alberghina L, Papa M. 2012. Targeting reactive astrogliosis by novel biotechnological strategies. Biotechnol Adv 30:261–271.

Crespo-López ME, Macêdo GL, Pereira SI, Arrifano GP, Picanço-Diniz DL, do Nascimento JL, Herculano AM. 2009. Mercury and human genotoxicity: critical considerations and possible molecular mechanisms. Pharmacol Res 60:212–220.

Crichton RR, Dexter DT, Ward RJ. 2008. Metal based neurodegenerative diseases: from molecular mechanisms to therapeutic strategies. Coordination Chem Rev 252:1189–1199.

Curle DC, Ray M, Persaud TV, Bertalanffy FD. 1987. Cytostatic action of methylmercuric chloride on mammalian duodenal cells. Histol Histopathol 2:223–226.

Dejana E, Colella S, Conforti G, Abbadini M, Gaboli M, Marchisio PC. 1988. Fibronectin and vitronectin regulate the organization of their respective Arg-Gly-Asp adhesion receptors in cultured human endothelial cells. J Cell Biol 107:1215–1223.

Farina M, Rocha JB, Aschner M. 2011a. Mechanisms of methylmercury-induced neurotoxicity: evidence from experimental studies. Life Sci 89: 555–563.

Farina M, Aschner M, Rocha JB. 2011b. Oxidative stress in MeHg-induced neurotoxicity. Toxicol Appl Pharmacol 256:405–4317.

Guttridge DC, Albanese C, Reuther JY, Pestell RG, Baldwin AS Jr. 1999. NF-kappaB controls cell growth and differentiation through transcriptional regulation of cyclin D1. Mol Cell Biol 19:5785–5799.

Hunter AM, Brown DL. 2000. Effects of microtubule-associated protein (MAP) expression on methylmercury-induced microtubule disassembly. Toxicol Appl Pharmacol 166:203–213.

Iwata-Ichikawa E, Kondo Y, Miyazaki I, Asanuma M, Ogawa N. 1999. Glial cells protect neurons against oxidative stress via transcriptional upregulation of the glutathione synthesis. J Neurochem 72:2334–2344.

Jomova K, Vondrakova D, Lawson M, Valko M. 2010. Metals, oxidative stress and neurodegenerative disorders. Mol Cell Biochem 345:91–104.

Kaminska B, Gozdz A, Zawadzka M, Ellert-Miklaszewska A, Lipko M. 2009. p38 MAPK signal transduction underlying brain inflammation and gliosis as therapeutic target. Anat Rec 292:1902–1913.

Kawano H, Kimura-Kuroda J, Komuta Y, Yoshioka N, Li HP, Kawamura K, Li Y, Raisman G. 2012. Role of the lesion scar in the response to damage and repair of the central nervous system. Cell Tissue Res 349:169–180.

Lin RC, Matesic DF, Marvin M, McKay RD, Brustle O. 1995. Re-expression of the intermediate filament nestin in reactive astrocytes. Neurobiol 2:79–85.

Malfa G, Tomasello B, Spatafora C, Cardile V, Scifo C, Tringali C, Renis M. 2010. Chemotherapeutic effects of resveratrol and its analogue 3,5,4′-trans-trimethoxystilbene on DU145. Trends Cancer Res 6: 45–54.

Murphy TH, Baraban SM. 1990. Glutamate toxicity in immature cortical neurons precedes development of glutamate receptor currents. Brain Res Dev Brain Res 57:146–150.

Ni M, Li X, Yin Z, Sidoryk-Wêgrzynowicz M, Jiang H, Farina M, Rocha JB, Syversen T, Aschner M. 2011. Comparative study on the response of rat primary astrocytes and microglia to methylmercury toxicity. Glia 59:810–820.

Norton WT, Aquino DA, Hozumi I, Chiu FC, Brosnan CF. 1992. Quantitative aspects of reactive gliosis: a review. Neurochem Res 17: 877–885.

O'Callaghan JP. 1993. Quantitative features of reactive gliosis following toxicant-induced damage of the CNS. Ann N Y Acad Sci 679:195–210.

Pekny M, Nilsson M. 2005. Astrocyte activation and reactive gliosis. Glia Rev 50:427–434.

Shanker G, Syversen T, Aschner M. 2003. Astrocyte-mediated methylmercury neurotoxicity. Biol Trace Elem Res 95:1–10.

Sofroniew MV, Vinters HV. 2010. Astrocytes: biology and pathology. Acta Neuropathol 119:7–35.

Sun GY, Xu J, Jensen MD, Simonyi A. 2004. Phospholipase A2 in the central nervous system: implications for neurodegenerative diseases. J Lipid Res 45:205–213.

Sun GY, Shelat PB, Jensen MB, He Y, Sun AY, Simonyi A. 2010. Phospholipases A2 and inflammatory responses in the central nervous system. Neuromol Med 12:133–148.

Tong W, Shah D, Xu J, Diehl JA, Hans A, Hannink M, Sun GY. 1999. Involvement of lipid mediators on cytokine signaling and induction of secretory phospholipase A2 in immortalized astrocytes (DITNC). J Mol Neurosci 12:89–99.

Villanueva EB, Little JP, Lambeau G, Klegeris A. 2012. Secreted phospholipase A2 group IIA is a neurotoxin released by stimulated human glial cells. Mol Cell Neurosci 49:430–438.

World Health Organization. 2010. Children's exposure to mercury compounds. Available from http://whqlibdoc.who.int/publications/2010/9789241500456_eng.pdf.

Wu J, Pajoohesh-Ganji A, Stoica BA, Dinizo M, Guanciale K, Faden AI. 2012. Delayed expression of cell cycle proteins contributes to astroglial scar formation and chronic inflammation after rat spinal cord contusion. J Neuroinflamm 9:169.

Yang K, Hitomi M, Stacey DW. 2006. Variations in cyclin D1 levels through the cell cycle determine the proliferative fate of a cell. Cell Division 18:32.